



**HAL**  
open science

## Nicotinic Receptor Subunits Atlas in the Adult Human Lung

Zania Diabasana, Jeanne-Marie Perotin, Randa Belgacemi, Julien Ancel, Pauline Mulette, Gonzague Delepine, Philippe Gosset, Uwe Maskos, Myriam Polette, Gaëtan Deslée, et al.

► **To cite this version:**

Zania Diabasana, Jeanne-Marie Perotin, Randa Belgacemi, Julien Ancel, Pauline Mulette, et al.. Nicotinic Receptor Subunits Atlas in the Adult Human Lung. *International Journal of Molecular Sciences*, 2020, 21 (20), pp.7446. 10.3390/ijms21207446 . pasteur-02975996

**HAL Id: pasteur-02975996**

**<https://pasteur.hal.science/pasteur-02975996>**

Submitted on 23 Oct 2020

**HAL** is a multi-disciplinary open access archive for the deposit and dissemination of scientific research documents, whether they are published or not. The documents may come from teaching and research institutions in France or abroad, or from public or private research centers.

L'archive ouverte pluridisciplinaire **HAL**, est destinée au dépôt et à la diffusion de documents scientifiques de niveau recherche, publiés ou non, émanant des établissements d'enseignement et de recherche français ou étrangers, des laboratoires publics ou privés.



Distributed under a Creative Commons Attribution 4.0 International License



Article

# Nicotinic Receptor Subunits Atlas in the Adult Human Lung

Zania Diabasana <sup>1</sup>, Jeanne-Marie Perotin <sup>1,2</sup>, Randa Belgacemi <sup>1</sup>, Julien Ancel <sup>1,2</sup> ,  
Pauline Mulette <sup>1,2</sup>, Gonzague Delepine <sup>1,3</sup>, Philippe Gosset <sup>4</sup> , Uwe Maskos <sup>5</sup>,  
Myriam Polette <sup>1,6</sup>, Gaëtan Deslée <sup>1,2</sup> and Valérian Dormoy <sup>1,\*</sup>

<sup>1</sup> Inserm UMR-S1250, P3Cell, University of Reims Champagne-Ardenne, SFR CAP-SANTE, 51092 Reims, France; zania.diabasana@inserm.fr (Z.D.); jmperotin-collard@chu-reims.fr (J.-M.P.); randa.belgacemi@univ-reims.fr (R.B.); jancel@chu-reims.fr (J.A.); pmulette@chu-reims.fr (P.M.); gdelepine@chu-reims.fr (G.D.); myriam.polette@univ-reims.fr (M.P.); gdeslee@chu-reims.fr (G.D.)

<sup>2</sup> Department of Respiratory Diseases, Centre Hospitalier Universitaire de Reims, Hôpital Maison Blanche, 51092 Reims, France

<sup>3</sup> Department of Thoracic Surgery, Centre Hospitalier Universitaire de Reims, Hôpital Maison Blanche, 51092 Reims, France

<sup>4</sup> CNRS UMR9017, Inserm U1019, University of Lille, Centre Hospitalier Régional Universitaire de Lille, Institut Pasteur, CIIL—Center for Infection and Immunity of Lille, 59000 Lille, France; philippe.gosset@pasteur-lille.fr

<sup>5</sup> Integrative Neurobiology of Cholinergic Systems, Institut Pasteur, CNRS UMR 3571, 75015 Paris, France; uwe.maskos@pasteur.fr

<sup>6</sup> Department of Biopathology, Centre Hospitalier Universitaire de Reims, Hôpital Maison Blanche, 51092 Reims, France

\* Correspondence: valerian.dormoy@univ-reims.fr; Tel.: +33-(0)3-10-73-62-28; Fax: +33-(0)3-26-06-58-61

Received: 17 September 2020; Accepted: 6 October 2020; Published: 9 October 2020



**Abstract:** Nicotinic acetylcholine receptors (nAChRs) are pentameric ligand-gated ion channels responsible for rapid neural and neuromuscular signal transmission. Although it is well documented that 16 subunits are encoded by the human genome, their presence in airway epithelial cells (AECs) remains poorly understood, and contribution to pathology is mainly discussed in the context of cancer. We analysed nAChR subunit expression in the human lungs of smokers and non-smokers using transcriptomic data for whole-lung tissues, isolated large AECs, and isolated small AECs. We identified differential expressions of nAChRs in terms of detection and repartition in the three modalities. Smoking-associated alterations were also unveiled. Then, we identified an nAChR transcriptomic print at the single-cell level. Finally, we reported the localizations of detectable nAChRs in bronchi and large bronchioles. Thus, we compiled the first complete atlas of pulmonary nAChR subunits to open new avenues to further unravel the involvement of these receptors in lung homeostasis and respiratory diseases.

**Keywords:** nicotinic receptors; airway epithelial cells; lung

## 1. Introduction

Nicotinic acetylcholine receptors (nAChRs) are ligand-gated (cation-permeable) proteins expressed in the brain and non-neuronal cells, including lung airway epithelial cells (AECs), macrophages, neutrophils, and muscle cells [1]. These receptors are composed of five subunits organized as homo- or hetero-pentamers forming a channel permeable to monovalent and divalent cations (predominantly Na<sup>+</sup>, K<sup>+</sup>, and Ca<sup>2+</sup>) [1,2]. There are 16 mammalian subunits, namely  $\alpha 1$ – $\alpha 7$ ,  $\alpha 9$ – $\alpha 10$ ,  $\beta 1$ – $\beta 4$ ,  $\delta$ ,  $\epsilon$ , and  $\gamma$  (the corresponding gene names are, respectively, CHRN (cholinergic receptors nicotinic subunits)

A1–A7, A9–A10, B1–B4, D, E, and G) [2]. Each subunit shares a common structure comprising a large amino-terminal segment (about 200 residues), four transmembrane domains TM1, TM2, TM3, and TM4 (less than 30 residues each), a large cytoplasmic loop (90 to 270 residues) localized between TM3 and TM4, and a variable carboxyl tail (10 to 30 residues) [2–4]. Muscle-type nAChRs are generally assembled from  $2(\alpha 1)/\beta 1/\delta/\gamma$  or  $2(\alpha 1)/\beta 1/\delta/\epsilon$  subtypes depending on muscle innervation [4–7]. Neuronal nAChRs are assembled from  $\alpha 2$ – $\alpha 7$ ,  $\alpha 9$ – $\alpha 10$ , and  $\beta 2$ – $\beta 4$  [8–10]. In the brain, homomeric  $\alpha 7$  and heteromeric  $\alpha 4/\beta 2$  subtypes are abundantly detected and are known to play an important role in memory and learning due to their predominance in the hippocampal and cortical neurons [11,12]. Other subtypes such as homomeric  $\alpha 9$ , heteromeric  $\alpha 2/\alpha 6$ ,  $\alpha 7/\beta 2$ , and  $\alpha 9/\alpha 10$  have also been detected to a lesser extent [1–3,12–18]. The diversity of nAChRs confers differential affinities to the ligands affecting several parameters, including the channel opening and closing duration, the modulation of ionic conductance, and cationic selectivity [1,2,12,14].

From a functional perspective, acetylcholine binding to nAChR at the extracellular interface between two subunits leads to an allosteric conformational change permitting the channel opening, followed by ion fluxes across the plasma membrane that participate in cell survival, differentiation, and proliferation [3,9,19,20]. Nicotine, one of the components of cigarette smoke, acts as an agonist implicated in the inhibition of apoptosis and oxidative stress responses, ultimately leading to lung impairments due to long-term exposure [4,21,22]. Although nicotinic receptors are ionotropic complexes, they may display metabotropic signalling properties via their association with trimeric GTP-binding proteins to regulate downstream pathways and cytokine expression [23,24].

Previous studies have established that multiple single-nucleotide nAChR polymorphisms are associated with risks of lung cancer and chronic obstructive pulmonary disease (COPD), highlighting their potential implication in respiratory diseases [19,25,26]. In addition, it has been hypothesized that the nAChRs may play a role in coronavirus disease 2019 (COVID-19) and might represent a therapeutic target, particularly regarding their potential contribution in the regulation of angiotensin-converting enzyme-2 (ACE-2), the main receptor for severe acute respiratory syndrome coronavirus (SARS-CoV-2) [27–29]. Altogether, this underlines the requirement of deciphering the atlas of pulmonary nAChR subunits.

Indeed, if the general expressions of muscle and neuronal nAChRs are well known, little information is available regarding their expression in the lung and particularly in different AECs [30]. Therefore, we conducted a transcriptomic and proteomic analysis of the localization and expression of all human nAChR subunits in the adult lung.

## 2. Results

### 2.1. Smoking-Associated Pulmonary nAChR Subunit Transcript Expressions

Considering the whole lung contains all types of tissues, including epithelia, muscle, connective, and nervous tissues (Figure 1a), the 16 nAChRs were detected among non-smoker subjects except for CHRNA7, which was consistent in both datasets containing non-smokers (Figure 1b and Supplemental Table S1). CHRNB1/E were very highly expressed; CHRNA6/A9/A10/B3/D were highly expressed (see Section 4). There was a significant increase in CHRNA1/A2/A7/B3/B4 transcript levels in smokers compared to non-smokers. Interestingly, CHRNA7 was only detected in smokers. On the contrary, CHRNA3/A4/A9/B2/D/G transcript levels were significantly decreased in smokers. The global repartition in non-smokers and smokers favoured CHRNA10/B1/E, representing almost half of all nAChR subunits expressed in lung tissues (Figure 1c and Supplemental Table S2). The differential repartitions of nAChRs between non-smokers and smokers matched their differential expressions.

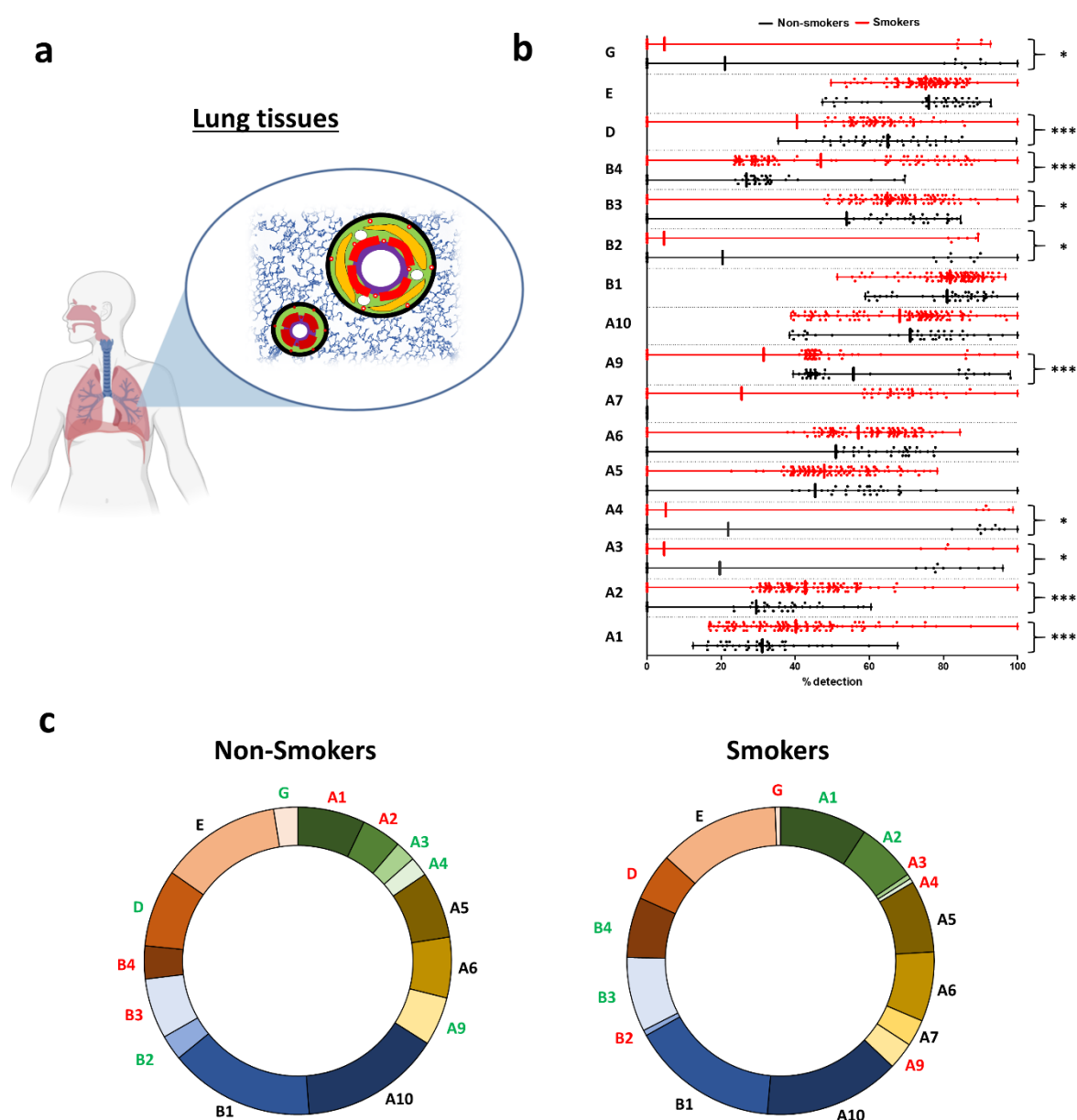


**Figure 1.** Evaluation of nicotinic acetylcholine receptor (nAChR) transcript levels in human lung tissues. (a) Illustration depicting the origin of the samples. Whole-lung tissues contained all the tissues present in the lung either in parenchyma or in/around bronchi and bronchioles. (b) Histogram showing the detection of nAChRs in non-smokers (black) and smokers (red). \*  $p < 0.05$ ; \*\*\*  $p < 0.001$  non-smokers ( $n = 42$ ) vs. smokers ( $n = 111$ ). (c) Pie charts showing the repartition of nAChRs in non-smokers (left) and smokers (right). Coloured subunits indicate upregulation (green) and downregulation (red) in both groups when statistically significant.

In large AEC (LAEC) (Figure 2a) CHRNA1/A2/A4/B1/B3/B4/D were not detected in non-smokers (Figure 2b and Supplemental Table S3). CHRNA5 was very highly expressed; CHRNA7/A10 were highly expressed. Interestingly, CHRNB1/B4 were only detected in smokers. There was a significant decrease in CHRNA5/A10 transcript levels in smokers when compared to non-smokers. The global repartition in non-smokers and smokers favoured CHRNA5/A7/A9/A10, representing more than 75% of all nAChRs expressed in LAEC (Figure 2c and Supplemental Table S4). There were no significant differences in terms of nAChR repartitions between non-smokers and smokers.

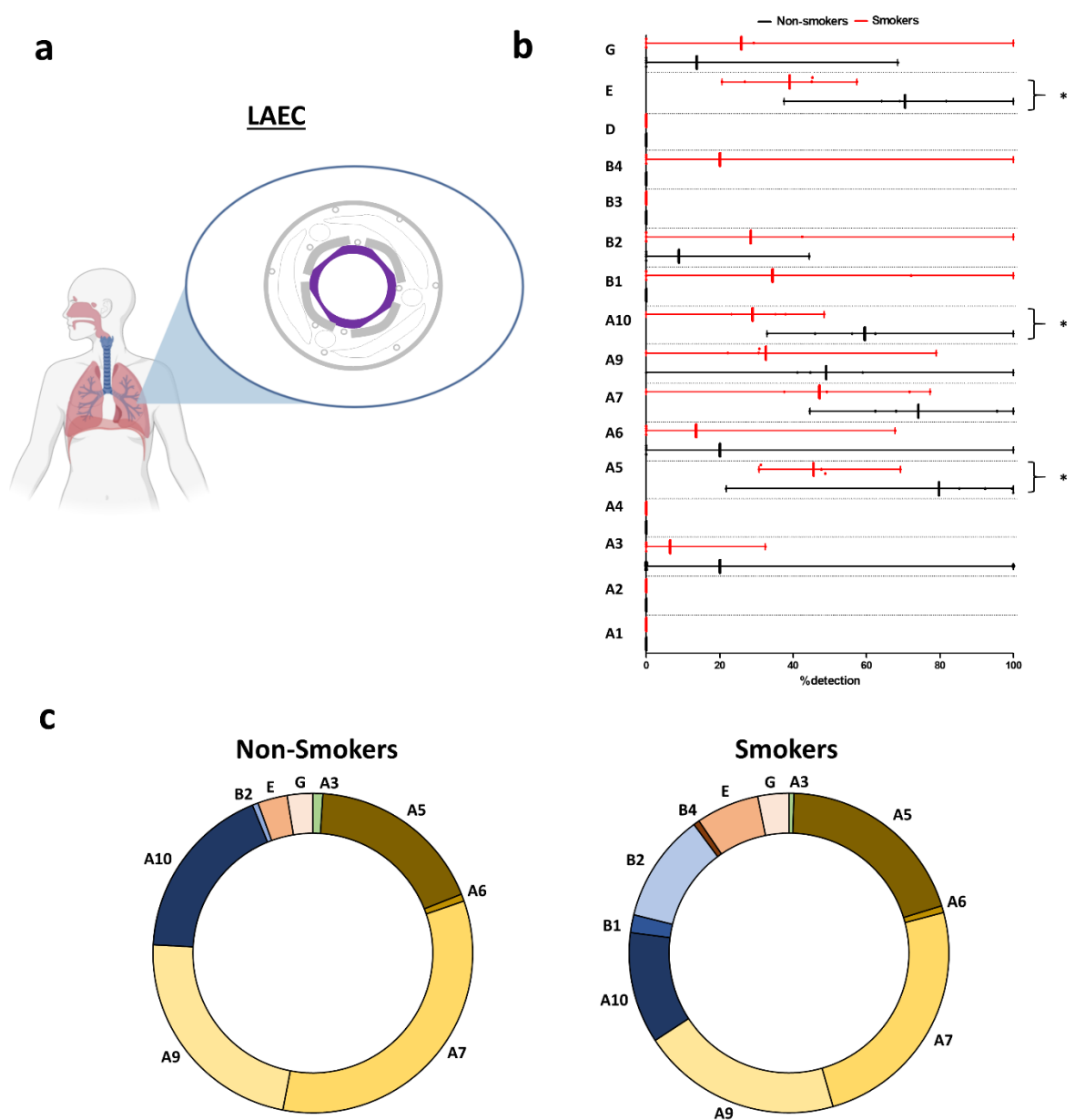


**Figure 2.** Evaluation of nAChR transcript levels in human large airway epithelial cells (LAECs). (a) Illustration depicting the origin of the samples. Isolated AECs were collected from bronchi. Large airway epithelial cells (LAECs) are depicted in purple. (b) Histogram showing the detection of nAChRs in non-smokers (black) and smokers (red). \*  $p < 0.05$  non-smokers ( $n = 5$ ) vs. smokers ( $n = 5$ ). (c) Pie charts showing the repartition of nAChRs in non-smokers (left) and smokers (right).

In small AEC (SAEC) (Figure 3a), the 16 nAChRs were detected among non-smokers with moderate or low expressions (Figure 3b and Supplemental Table S5). There was a significant increase in CHRNA5/A7/B2/B3 transcript levels in smokers compared to non-smokers. The global repartition in non-smokers and smokers favoured CHRNA7/A9/A10/B2, representing half of the nAChRs expressed in SAEC (Figure 3c and Supplemental Table S6). There was a significant increase in CHRNA7/B2/B3 and a significant decrease in CHRNA2/A9 in the repartition of nAChRs in smokers compared to non-smokers.

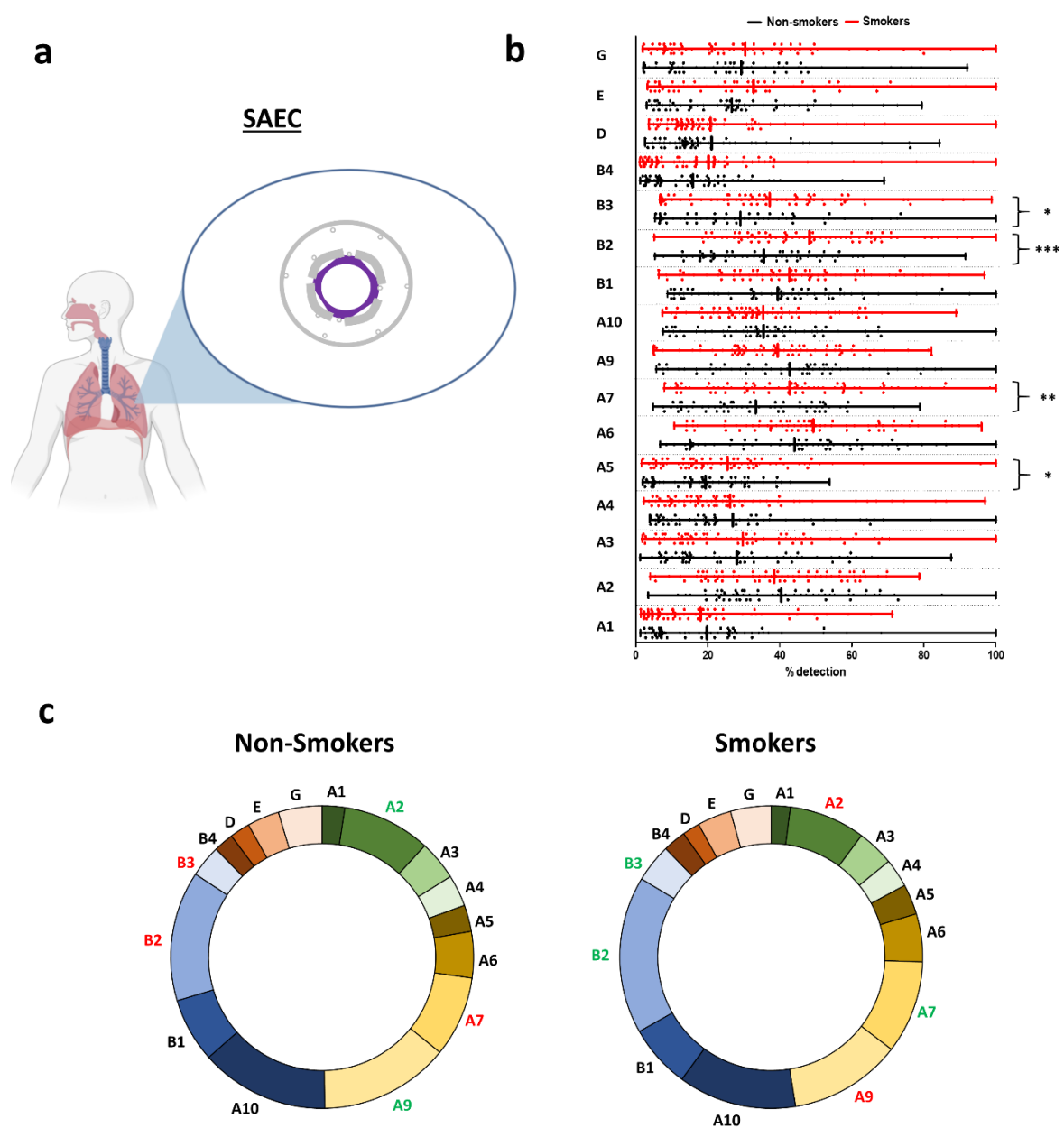


**Figure 3.** Evaluation of nAChR transcript levels in human small airway epithelial cells (SAECs). (a) Illustration depicting the origin of the samples. Isolated AECs were collected from bronchioles. Small airway epithelial cells (SAECs) are depicted in purple. (b) Histograms showing the detection of nAChRs in non-smokers (black) and smokers (red). \*  $p < 0.05$ ; \*\*  $p < 0.01$ ; \*\*\*  $p < 0.001$  non-smokers ( $n = 63$ ) vs. smokers ( $n = 72$ ). (c) Pie charts showing the repartition of nAChRs in non-smokers (left) and smokers (right). Coloured subunits indicate upregulation (green) and downregulation (red) in both groups when statistically significant.

### 2.2. Differential Pulmonary nAChRs Transcript Expressions at the Single-Cell Scale

At the level of single-cell transcriptomes (Figure 4), *CHRNA5/A7/A9/A10/B1/E* were highly expressed in most of the AEC populations including alveolar, basal, goblet, multiciliated, and club cells. *CHRNA1/A2/A4/A6/B2/B3/D/G* showed low to no expression in AEC. Interestingly, functional AEC cell populations were distinguished with their nAChR signatures: pneumocytes expressed *CHRNA5/A10/B1*; basal cells expressed *CHRNA5/A7/A10/B1/E*; goblet cells expressed *CHRNA7/A10/B1/E*; multiciliated cells expressed *CHRNA9/10/B1/E*; club cells expressed *CHRNA7/A10/B1*; ionocytes expressed *CHRNA3/B4/E*.

Considering non-epithelial cells, CHRNA1/A3/A5/A10/B1/E were highly expressed in specific populations of immune cells including macrophages, B cells, dendritic cells, and mast cells. CHRNB1 expression was specific to lymphatic cells. CHRNA5/B1/E were highly expressed in fibroblasts; CHRNA3/A10/B1 in smooth muscle cells; CHRNA5/B1/E in endothelial cells and macrophages. B cells and dendritic cells mainly expressed CHRNB1/E.

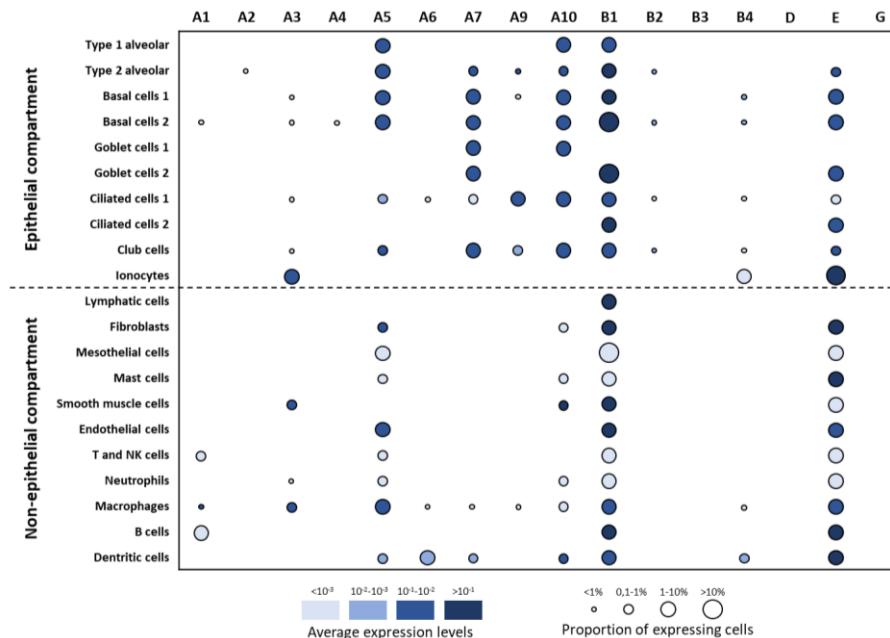
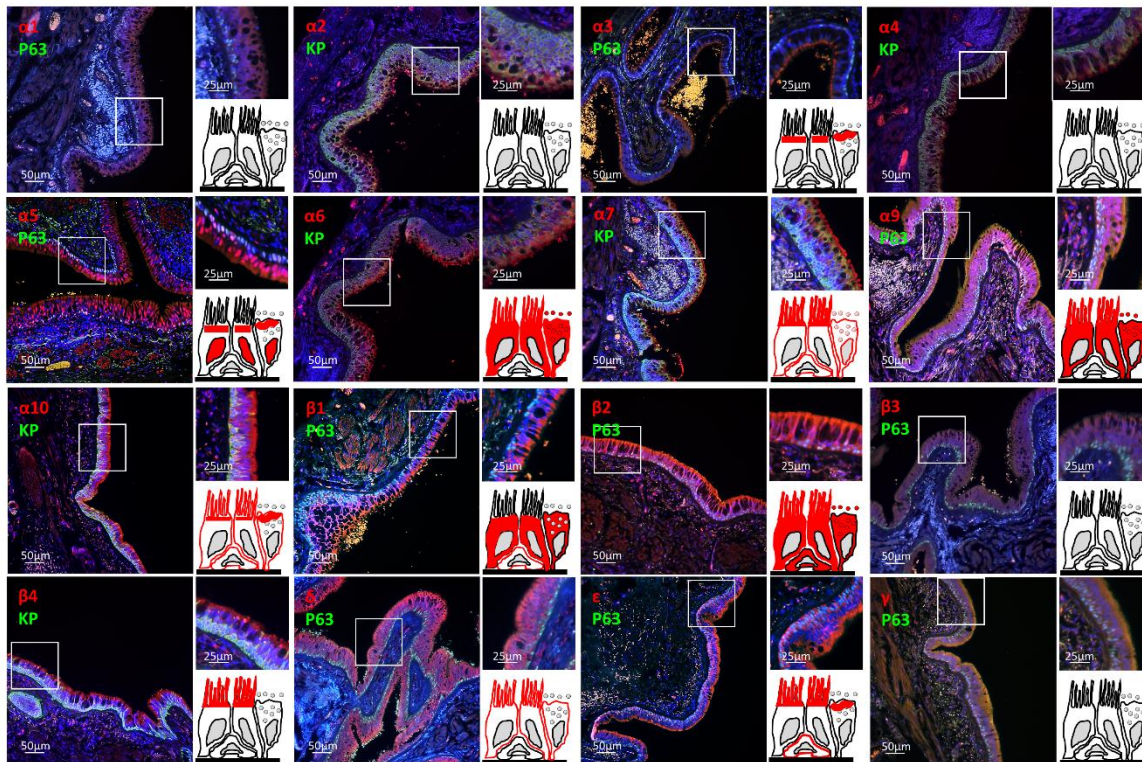


**Figure 4.** Evaluation of nAChR expressions in lung single-cell populations. Dot plots of nAChR expressions in the epithelial and non-epithelial compartments. The identities of cell populations are shown on the y-axis, and the subunits on the x-axis. The colour intensity represents the average expression level, and the size of the dots represents the proportion of the expressing cells in each population. Raw expression values were normalized, log-transformed, and summarized by published cell clustering.

### 2.3. Identification of nAChR Subunits in Bronchial and Large Bronchiolar Epithelia

To investigate nAChR subunit localization in the lung, we selected commercially available validated primary antibodies displaying the antigenic sequences demonstrating the lowest percentage of identity with regard to cross-reactivity (Supplemental Tables S7 and S8; Supplemental Figures S1 and S2). We focussed here on bronchi and large bronchioles as well as smooth muscle and blood vessels on formalin-fixed paraffin-embedded (FFPE) tissues (Figure 5a,b). Subunits  $\alpha 1/\alpha 2/\alpha 4/\beta 3/\gamma$  were not detected. Subunit  $\alpha 3$  seemed restricted to the apical side of differentiated cells. Surprisingly,  $\alpha 5$  was systematically found in AEC nuclei and the apical side of differentiated AECs, while its pattern was consistent with membrane-bound receptors on smooth muscle cells. Subunits  $\alpha 6$  and  $\alpha 9$  presented similar staining in differentiated AECs, such as  $\alpha 7/\alpha 10/\beta 1/\beta 2/\delta/\epsilon$ , which in addition were found in non-differentiated AECs. Finally,  $\beta 4$  appeared in multiciliated cells only. When available, our observations were generally concordant with the data from the Human Protein Atlas (Figure 5b and Supplemental Figure S3).

a



b

nAChR	Lung localization (S, B, b*)	Cell population	Subcellular localization	Human protein atlas lung detection
$\alpha 1$	-	-	-	-
$\alpha 2$	-	-	-	NA
$\alpha 3$	B, b	Multiciliated and goblet cells	Sub-cilia, apical	Multiciliated cells
$\alpha 4$	-	-	-	NA
$\alpha 5$	S, B, b	Multiciliated, goblet and basal cells Smooth muscle	Epithelial cell nuclei, apical myoepithelial cell membrane	-
$\alpha 6$	B, b	Multiciliated, goblet cells	Cilia, membrane, cytoplasm	NA
$\alpha 7$	S, B, b	Multiciliated, goblet and basal cells Smooth muscle	Cilia, membrane	Multiciliated, goblet, and basal cells
$\alpha 9$	B, b	Multiciliated and goblet cells	Cilia, cytoplasm	NA
$\alpha 10$	S, B, b	Multiciliated, goblet and basal cells Smooth muscle cells	Cilia, membrane	NA
$\beta 1$	S, B, b	Multiciliated, goblet and basal cells Blood vessels, Smooth muscles	Cytoplasm	Multiciliated and basal cell
$\beta 2$	B, b	Multiciliated, goblet and basal cells	Cilia, cell membrane	NA
$\beta 3$	-	-	-	-
$\beta 4$	B, b	Multiciliated cells	Cilia	NA
$\delta$	B, b	Multiciliated and goblet cells	Cell membrane, cilia	NA
$\epsilon$	B, b	Multiciliated, goblet and basal cells	Cell membrane	NA
$\gamma$	-	-	-	NA

\* S, stroma; B, bronchi; b, large bronchioles

**Figure 5.** nAChR localizations in human respiratory epithelia. (a) Representative micrographs showing the bronchial epithelia on formalin-fixed paraffin-embedded (FFPE) lung tissues stained for the nAChRs (all red), non-differentiated cells (p63 or pan-cytokeratin, green), and cell nuclei (DAPI, blue). Magnification corresponding to the selected area is shown. Drawings depict the localization of each nAChR subunit (in red). (b) Table summarizing nAChR subunit cellular and sub-cellular localization and the available microscopic data from the Human Protein Atlas (<https://www.proteinatlas.org/>). NA, not available; -, no detection.

### 3. Discussion

This is the first study showing transcript levels and localizations of all nAChR subunits in the human adult lung. Interestingly, we identified distinct variations in terms of nAChR transcript levels between whole-lung tissues, LAEC, and SAEC, as well as important changes between non-smokers and smokers. Since whole-lung transcriptomics encompasses all pulmonary tissues, isolated cell studies represent the ideal strategy to unveil nAChR functions in airways. It has been successfully implemented in the context of AEC differentiation analysis, asthma, and idiopathic pulmonary fibrosis [31–35]. If they summarize the transcriptomic profile of the organ, whole-lung microarray data require tissue or single-cell analyses to distinguish the contribution of each cellular population to the specific gene expression. Otherwise, it would be admitted that a gene is ubiquitously expressed in the lung, while it is only found in one histological tissue. As such, our comparative analysis pointed mainly towards CHRNA5/A7/A10/B2/B3 to tackle the association of nAChR expression and smoking. Furthermore, the impact of smoking could be tied into the associated risks of respiratory diseases, provided complete clinical data are available.

We included in the analysis of nAChR expression levels 298 subjects in three distinct modalities (whole-lung tissues, LAEC, and SAEC) and performed a preliminary identification of single-cell transcriptomic signature. Our immunostaining analyses provided important data regarding the subcellular localization of nAChR subunits in bronchi and large bronchioles. Microscopic observations and transcriptomic analysis were generally concordant. Because of their modalities of association at the cell membrane and their high degree of amino acids identity, nAChR immunostainings were generally sparse, rarely concordant, and performed on murine tissues in the literature [30,36–38]. A careful validation method including heterologous cells overexpressing the different human nAChR subtypes is required to further validate all subunit nAChR antibodies in the human adult lung [39]. Nonetheless, since we selected all our antibodies based on thorough sequence alignments of the antigenic sequences, we provided here a complete description of all nAChRs in bronchi and large bronchioles. Only individual subunits were detected and not the receptors, which are assembled of five subunits; *in vitro* experimental studies will be required to confirm the presence of various pentamers at the cell surface of the lung tissues. Other caveats complicating the identification of nAChRs include their dynamic of assembly/recycling at the cell surface [7,40] and their differential requirement according to the cellular context (quiescence, proliferation, oxidative stress, etc.) [1].

Additional studies on larger cohorts are needed to complement and refine our analysis. Deciphering the cellular and molecular impact of the observed differences in transcript expressions in the context of smoking will be essential to understanding nAChR-associated pathogenesis. It will be particularly insightful for at least three lung diseases where smoking may partly impact homeostasis: lung cancers, COPD, and COVID-19. (i) nAChR single-nucleotide polymorphisms (SNPs) were associated with lung cancer cells [41,42], and nAChRs were shown to be involved in cancer cell proliferation and survival [43–46]. Interestingly, several subunits (including  $\alpha 5$ -7-10/ $\beta 2$ -3) were identified in cancer cell lines, and selective nAChR inhibitors induced anti-tumour effects [47,48]. In addition, acetylcholine-signalling proteins were involved in the progression of lung cancer [49]. Altogether, understanding the repartition and the possible assembly of nAChRs at the cancer cell surface may pave the way towards the design of effective anti-cancer drugs. (ii) nAChR SNPs were also associated with nicotine dependence and COPD [50–54]. CHRNA3/A5/B4 polymorphisms were heavily discussed in the dissection of the genetic origins of COPD, but no functional studies have been published so far [55]. In addition,  $\alpha 7$  and its ligands received particular attention as potential inflammatory players in COPD patients [54,56]. Exploring the involvement of nAChRs in COPD pathogenesis and progression in light of their differential distribution in lung cell populations may help improve health care for this pathology lacking treatments. (iii) Nicotine, an exogenous ligand of nAChRs and, more generally, smoking, have been shown *in vitro* and *in vivo* to modulate the expression of hACE2, the main receptor of the SARS-CoV-2 spike S protein [57–60]. In light of the

differential subunit expressions, it will be of interest to analyze the localizations of hACE2 and nAChRs in COVID-19 tissues.

We provided the first atlas of nAChR subunits in the lung and invited cartographers to complete the map in order to provide a fundamental understanding of these crucial actors of homeostasis that may contribute to chronic and acute respiratory diseases. The identification of each potential subunit that may assemble functional channels at the cell surface is a requisite for the optimal design of efficient pharmacological modulations of nAChRs in the context of the pharmacology of the respiratory system.

## 4. Materials and Methods

### 4.1. Human Subjects

Patients scheduled for lung resection for cancer (University Hospital of Reims, France) were prospectively recruited ( $n = 10$ ) following standards established and approved by the institutional review board of the University Hospital of Reims, France (IRB Reims-CHU, date of approval: 12 June 2011). In addition, 10 patients who underwent a routine large airway fiberoptic bronchoscopy with bronchial brushings under local anaesthesia according to international guidelines were also recruited (5 non-smokers, 5 smokers) [61]. Informed consent was obtained from all the patients. Subjects were recruited from the Department of Pulmonary Medicine at the University Hospital of Reims (France) and included in the cohort for Research and Innovation in Chronic Inflammatory Respiratory Diseases (RINNOPARI, NCT02924818). The study was approved by the ethics committee for the protection of human beings involved in biomedical research (CCP Dijon EST I, N°2016-A00242-49, date of approval: 31 May 2016) and was conducted in accordance with the ethical guideline of the Declaration of Helsinki. Patients with chronic obstructive pulmonary disease, asthma, cystic fibrosis, bronchiectasis, or pulmonary fibrosis were excluded. At inclusion, age, sex, smoking history, and pulmonary function test results were recorded to exclude patients with an alteration of lung functions. Ex-smokers were considered for a withdrawal longer than 5 years.

### 4.2. Sample Processing

Fresh airway epithelial cells (AECs) obtained from bronchial brushings (right lower lobe, 5th to 8th divisions) were suspended for 30 min in Roswell Park Memorial Institute Medium (RPMI) (1% penicillin/streptomycin + 10% Bovine Serum Albumin (BSA)) before centrifugation (13,500g  $\times$  2 times). The cell pellet was dissociated in 1 mL of Trypsin Versene (Lonza), centrifuged (13,500g  $\times$  2 times), and kept at  $-20$  °C until further steps.

### 4.3. RT-qPCR Analyses

Total RNA from AEC bronchial brushings was isolated by a High Pure RNA isolation kit (Roche Diagnostics), and 250 ng was reverse-transcribed into cDNA by a Transcriptor First Stand cDNA Synthesis kit (Roche Diagnostics, Meylan, France). Quantitative PCR reactions were performed with a Fast Start Universal Probe Master kit and UPL-probe system in a LightCycler 480 Instrument (Roche Diagnostics) as recommended by the manufacturer. Primers listed in Supplementary Table S9 were designed via the Universal Probe Library Assay Design Center (Roche, Mannheim, Germany). Results for all expression data regarding transcripts were normalized to the expression of the house-keeping gene GAPDH amplified with the following primers: forward 5'-ACCAGGTGGTCTCCTCTGAC-3', reverse 5'-TGCTGTAGCCAAATTCGTTG-3'. We verified that GAPDH transcript detection levels were highly similar between non-smokers and smokers to validate the housekeeping gene (average Ct =  $25.54 \pm 0.17$  in non-smokers vs.  $25.35 \pm 0.34$  in smokers;  $p = 0.64$ ). Relative gene expression was assessed by the  $\Delta\Delta$ Ct method [62] and expressed as  $2^{-\Delta\Delta$ Ct}. To compare data generated via PCR with RNAseq analysis, we transformed the transcript expressions to a percentage scale considering the highest and lowest values per subunit for the detection, or across all the subunits for the repartition.

#### 4.4. Immunofluorescent Staining and Analyses

Immunohistochemistry was performed on formalin-fixed paraffin-embedded (FFPE) lung tissues distant from the tumour as previously described [63]. Only patients having no respiratory diseases were included (smokers and ex-smokers). Five micrometer sections were processed for hematoxylin and eosin staining and observed on a microscope ( $\times 20$ ) to confirm the presence of bronchi and large bronchioles (pseudostratified epithelia). The bronchial epithelium was analysed on the entire slide including 2 to 7 units per patient. FFPE lung tissue section slides were deparaffinised and blocked with 10% BSA in phosphate-buffered saline (PBS) for 30 min at room temperature. Tissue sections were then incubated with the primary antibodies as listed in Supplementary Table S7 for one night at 4 °C in 3% BSA in PBS. After the PBS wash, a second primary antibody was used to highlight non-differentiated cells on epithelia for 2h at room temperature: p63 (AF1916, 1:200, R&D Systems, Noyal Châtillon sur Seiche, France) or pan-cytokeratin (CK, 1:1000, E-AB-33599, Elabscience, Clinisciences, Nanterre, France). Sections were washed with PBS and incubated with the appropriate secondary antibodies in 3% BSA in PBS for 30 min at room temperature: Alexa Fluor<sup>®</sup> (Invitrogen, Fisherscientific, Illkirch, France) donkey anti-rabbit IgG 594 (A21207), donkey anti-goat IgG 488 (A11055), goat anti-mouse IgG 594 (A11005), and goat anti-rabbit IgG 488 (A11008). DNA was stained with DAPI during incubation with the secondary antibodies. Micrographs were acquired on a Zeiss AxioImageur (20 $\times$  Ph) with ZEN software (8.1, 2012) and processed with ImageJ (National Institutes of Health) for analysis. For each patient, five random fields per section containing bronchi and large bronchioles were taken to evaluate the localization of nicotinic receptors on epithelial and stromal cells. We selected the most suitable primary antibodies directed against each subunit, considering external validations, identity, and staining optimization, to highlight the localization of nAChRs on bronchi and large bronchioles.

#### 4.5. Transcriptome Profiling Microarray Analysis

Gene expressions of non-smoking and smoking subjects with no chronic respiratory diseases were collected from datasets available online (GEO database; <http://www.ncbi.nlm.nih.gov/geo>) including whole-lung tissue samples in 153 subjects (42 non-smokers, 111 smokers; GSE103174, 76925, and 47460) or small airway bronchoscopic samples (10th to 14th divisions) in 135 subjects (63 non-smokers, 72 smokers; GSE11784).

In order to compare transcriptomic data extracted from various datasets or PCR reactions, we formatted the absolute values to a percentage scale. Concerning the detection of genes, we first identified for each gene the highest and lowest expression values in both non-smokers and smokers to set the maximal value at 100%. After proportionally expressing each of the single expression values for all the subunits, the average was calculated and plotted on a graph. To discuss the relative level of expressions, we arbitrarily categorized 4 groups: (1) very high expressions, the average percentage of expression is over 75% of the maximum; (2) high expressions, the average percentage of expression is between 50 and 75% of the maximum; (3) moderate expressions, the average percentage of expression is between 25 and 50% of the maximum; (4) and low expression, the average percentage of expression is below 25% of the maximum. Concerning the repartition, the total expressions of absolute values for all nAChR were summed for each patient of the considered dataset to express the proportion of each subunit. The comparative average percentage of expression of each subunit for all patients was plotted in a pie chart.

#### 4.6. Single-Cell Sequencing

The published dataset can be found at [lungcellatlas.org](http://lungcellatlas.org) and <https://www.covid19cellatlas.org>. We retained cell clustering based on the original studies and considered only lung samples (brushing and parenchyma from resected tissues) from subjects with no respiratory disease [33]. An Illumina HiSeq 4000 per 10 $\times$  Genomics chip position was used ( $n = 6$ ; 2000–5000 cells/sample). Additional sequencing was performed to obtain coverage, or at least mean coverage, of 100,000 reads per cell.

#### 4.7. Statistics

The data are expressed as mean values and percentages. Differences between the two groups (non-smokers and smokers) for each gene were determined using the Student *t* test. A *p*-value < 0.05 was considered significant; \*, *p* < 0.05; \*\*, *p* < 0.01; \*\*\*, *p* < 0.001.

**Supplementary Materials:** Supplementary materials can be found at <http://www.mdpi.com/1422-0067/21/20/7446/s1>.

**Author Contributions:** Conceptualization, V.D.; methodology, V.D.; formal analysis, Z.D., J.-M.P., M.P., P.G., U.M., G.D. (Gaëtan Deslée) and V.D.; investigation, Z.D., R.B. and V.D.; resources, J.-M.P., J.A., P.M., G.D. (Gonzague Delepine) and G.D. (Gaëtan Deslée); data curation, J.-M.P., J.A., P.M. and G.D. (Gaëtan Deslée); writing—original draft preparation, Z.D. and V.D.; writing—review and editing, Z.D., J.-M.P., M.P., P.G., U.M., G.D. (Gaëtan Deslée) and V.D.; supervision, G.D. (Gaëtan Deslée) and V.D.; project administration, V.D.; funding acquisition, P.G., U.M., G.D. (Gaëtan Deslée) and V.D. All authors have read and agreed to the published version of the manuscript.

**Funding:** This work was supported by funding from the University of Reims Champagne-Ardenne (URCA), the French National Institute of Health and Medical Research (Inserm) and a grant from the Research Institute in Public Health (IReSP) in association with the National Institute of Cancer (INCa). It was carried out in the framework of the Federative Research Structure CAP-Santé and benefited from the Project Research and Innovation in Inflammatory Respiratory Diseases (RINNOPARI).

**Acknowledgments:** We thank the members of the Inserm UMR-S 1250 unit and our collaborators for their helpful comments and insights. We thank the Platform of Cell and Tissue Imaging (PICT) for technical assistance. The drawings were created with BioRender.com.

**Conflicts of Interest:** G.D. (Gaëtan Deslée) reports personal fees from Nuvaira, personal fees from BTG/PneumRx, personal fees from Chiesi, personal fees from Boehringer, personal fees from Astra Zeneca, outside the submitted work. V.D. reports personal fees from Chiesi outside the submitted work. The funders had no role in the design of the study; in the collection, analyses, or interpretation of data; in the writing of the manuscript, or in the decision to publish the results.

#### Abbreviations

nAChRs	Nicotinic acetylcholine receptors
AEC	Airway epithelial cells
COPD	Chronic obstructive pulmonary disease
COVID-19	Coronavirus disease 2019
ACE-2	Angiotensin-converting enzyme-2
SARS-CoV-2	Severe acute respiratory syndrome coronavirus
FFPE	Formalin-fixed paraffin-embedded
LAEC	Large airway epithelial cell
SAEC	Small airway epithelial cell
SNP	Single-nucleotide polymorphisms
RAS	Renin–angiotensin system

#### References

- Zoli, M.; Pucci, S.; Vilella, A.; Gotti, C. Neuronal and Extraneuronal Nicotinic Acetylcholine Receptors. *Curr. Neuropharmacol.* **2018**, *16*, 338–349. [[CrossRef](#)] [[PubMed](#)]
- Dani, J.A. Neuronal Nicotinic Acetylcholine Receptor Structure and Function and Response to Nicotine. *Int. Rev. Neurobiol.* **2015**, *124*, 3–19. [[CrossRef](#)] [[PubMed](#)]
- Gündisch, D.; Eibl, C. Nicotinic acetylcholine receptor ligands, a patent review (2006–2011). *Expert Opin. Ther. Pat.* **2011**, *21*, 1867–1896. [[CrossRef](#)]
- Grando, S.A. Connections of nicotine to cancer. *Nat. Rev. Cancer* **2014**, *14*, 419–429. [[CrossRef](#)] [[PubMed](#)]
- Grassi, F.; Fucile, S. Calcium influx through muscle nAChR-channels: One route, multiple roles. *Neuroscience* **2019**, *439*, 117–124. [[CrossRef](#)] [[PubMed](#)]
- Conti-Tronconi, B.M.; McLane, K.E.; Raftery, M.A.; Grando, S.A.; Protti, M.P. The nicotinic acetylcholine receptor: Structure and autoimmune pathology. *Crit. Rev. Biochem. Mol. Biol.* **1994**, *29*, 69–123. [[CrossRef](#)]
- Rudolf, R.; Straka, T. Nicotinic acetylcholine receptor at vertebrate motor endplates: Endocytosis, recycling, and degradation. *Neurosci. Lett.* **2019**, *711*, 134434. [[CrossRef](#)]

8. Kabbani, N.; Nichols, R.A. Beyond the Channel: Metabotropic Signaling by Nicotinic Receptors. *Trends Pharmacol. Sci.* **2018**, *39*, 354–366. [[CrossRef](#)]
9. Papke, R.L.; Lindstrom, J.M. Nicotinic acetylcholine receptors: Conventional and unconventional ligands and signaling. *Neuropharmacology* **2020**, *168*, 108021. [[CrossRef](#)]
10. Albuquerque, E.X.; Pereira, E.F.R.; Alkondon, M.; Rogers, S.W. Mammalian nicotinic acetylcholine receptors: From structure to function. *Physiol. Rev.* **2009**, *89*, 73–120. [[CrossRef](#)]
11. Baranowska, U.; Wiśniewska, R.J. The  $\alpha$ 7-nACh nicotinic receptor and its role in memory and selected diseases of the central nervous system. *Postepy. Hig. Med. Dosw. (Online)* **2017**, *71*, 633–648. [[CrossRef](#)]
12. Bertrand, D.; Terry, A.V. The wonderland of neuronal nicotinic acetylcholine receptors. *Biochem. Pharmacol.* **2018**, *151*, 214–225. [[CrossRef](#)]
13. Crespi, A.; Colombo, S.F.; Gotti, C. Proteins and chemical chaperones involved in neuronal nicotinic receptor expression and function: An update. *Br. J. Pharmacol.* **2018**, *175*, 1869–1879. [[CrossRef](#)]
14. Medjber, K.; Freidja, M.L.; Grelet, S.; Lorenzato, M.; Maouche, K.; Nawrocki-Raby, B.; Birembaut, P.; Polette, M.; Tournier, J.-M. Role of nicotinic acetylcholine receptors in cell proliferation and tumour invasion in broncho-pulmonary carcinomas. *Lung Cancer* **2015**, *87*, 258–264. [[CrossRef](#)]
15. Koukoulis, F.; Rooy, M.; Changeux, J.-P.; Maskos, U. Nicotinic receptors in mouse prefrontal cortex modulate ultraslow fluctuations related to conscious processing. *Proc. Natl. Acad. Sci. USA* **2016**, *113*, 14823–14828. [[CrossRef](#)]
16. Changeux, J.-P.; Corringier, P.-J.; Maskos, U. The nicotinic acetylcholine receptor: From molecular biology to cognition. *Neuropharmacology* **2015**, *96*, 135–136. [[CrossRef](#)]
17. Le Novère, N.; Corringier, P.-J.; Changeux, J.-P. The diversity of subunit composition in nAChRs: Evolutionary origins, physiologic and pharmacologic consequences. *J. Neurobiol.* **2002**, *53*, 447–456. [[CrossRef](#)]
18. Wu, J.; Liu, Q.; Tang, P.; Mikkelsen, J.D.; Shen, J.; Whiteaker, P.; Yakel, J.L. Heteromeric  $\alpha$ 7 $\beta$ 2 Nicotinic Acetylcholine Receptors in the Brain. *Trends Pharmacol. Sci.* **2016**, *37*, 562–574. [[CrossRef](#)]
19. Chen, J.; Cheuk, I.W.Y.; Shin, V.Y.; Kwong, A. Acetylcholine receptors: Key players in cancer development. *Surg. Oncol.* **2019**, *31*, 46–53. [[CrossRef](#)]
20. Maouche, K.; Polette, M.; Jolly, T.; Medjber, K.; Cloëz-Tayarani, I.; Changeux, J.-P.; Burlet, H.; Terryn, C.; Coraux, C.; Zahm, J.-M.; et al.  $\alpha$ 7 nicotinic acetylcholine receptor regulates airway epithelium differentiation by controlling basal cell proliferation. *Am. J. Pathol.* **2009**, *175*, 1868–1882. [[CrossRef](#)]
21. Munakata, S.; Ishimori, K.; Kitamura, N.; Ishikawa, S.; Takanami, Y.; Ito, S. Oxidative stress responses in human bronchial epithelial cells exposed to cigarette smoke and vapor from tobacco- and nicotine-containing products. *Regul. Toxicol. Pharmacol.* **2018**, *99*, 122–128. [[CrossRef](#)] [[PubMed](#)]
22. Herman, M.; Tarran, R. E-cigarettes, nicotine, the lung and the brain: Multi-level cascading pathophysiology. *J. Physiol.* **2020**, JP278388. [[CrossRef](#)]
23. Kabbani, N.; Nordman, J.C.; Corgiat, B.A.; Veltri, D.P.; Shehu, A.; Seymour, V.A.; Adams, D.J. Are nicotinic acetylcholine receptors coupled to G proteins? *Bioessays* **2013**, *35*, 1025–1034. [[CrossRef](#)]
24. King, J.R.; Ullah, A.; Bak, E.; Jafri, M.S.; Kabbani, N. Ionotropic and Metabotropic Mechanisms of Allosteric Modulation of  $\alpha$ 7 Nicotinic Receptor Intracellular Calcium. *Mol. Pharmacol.* **2018**, *93*, 601–611. [[CrossRef](#)]
25. Cui, K.; Ge, X.; Ma, H. Four SNPs in the CHRNA3/5 alpha-neuronal nicotinic acetylcholine receptor subunit locus are associated with COPD risk based on meta-analyses. *PLoS ONE* **2014**, *9*, e102324. [[CrossRef](#)]
26. Maskos, U. The nicotinic receptor alpha5 coding polymorphism rs16969968 as a major target in disease: Functional dissection and remaining challenges. *J. Neurochem.* **2020**. [[CrossRef](#)]
27. Sriram, K.; Insel, P.A. A hypothesis for pathobiology and treatment of COVID-19: The centrality of ACE1/ACE2 imbalance. *Br. J. Pharmacol.* **2020**, bph.15082. [[CrossRef](#)]
28. Oakes, J.M.; Fuchs, R.M.; Gardner, J.D.; Lazartigues, E.; Yue, X. Nicotine and the renin-angiotensin system. *Am. J. Physiol. Regul. Integr. Comp. Physiol.* **2018**, *315*, R895–R906. [[CrossRef](#)]
29. Changeux, J.-P.; Amoura, Z.; Rey, F.A.; Miyara, M. A nicotinic hypothesis for Covid-19 with preventive and therapeutic implications. *Comptes Rendus Biol.* **2020**, *343*, 33–39. [[CrossRef](#)]
30. Lam, D.C.-L.; Luo, S.Y.; Fu, K.-H.; Lui, M.M.-S.; Chan, K.-H.; Wistuba, I.I.; Gao, B.; Tsao, S.-W.; Ip, M.S.-M.; Minna, J.D. Nicotinic acetylcholine receptor expression in human airway correlates with lung function. *Am. J. Physiol. Lung Cell. Mol. Physiol.* **2016**, *310*, L232–L239. [[CrossRef](#)]

31. Reyfman, P.A.; Walter, J.M.; Joshi, N.; Anekalla, K.R.; McQuattie-Pimentel, A.C.; Chiu, S.; Fernandez, R.; Akbarpour, M.; Chen, C.-I.; Ren, Z.; et al. Single-Cell Transcriptomic Analysis of Human Lung Provides Insights into the Pathobiology of Pulmonary Fibrosis. *Am. J. Respir. Crit. Care Med.* **2019**, *199*, 1517–1536. [[CrossRef](#)] [[PubMed](#)]
32. Schiller, H.B.; Montoro, D.T.; Simon, L.M.; Rawlins, E.L.; Meyer, K.B.; Strunz, M.; Vieira Braga, F.A.; Timens, W.; Koppelman, G.H.; Budinger, G.R.S.; et al. The Human Lung Cell Atlas: A High-Resolution Reference Map of the Human Lung in Health and Disease. *Am. J. Respir. Cell Mol. Biol.* **2019**, *61*, 31–41. [[CrossRef](#)] [[PubMed](#)]
33. Vieira Braga, F.A.; Kar, G.; Berg, M.; Carpaij, O.A.; Polanski, K.; Simon, L.M.; Brouwer, S.; Gomes, T.; Hesse, L.; Jiang, J.; et al. A cellular census of human lungs identifies novel cell states in health and in asthma. *Nat. Med.* **2019**, *25*, 1153–1163. [[CrossRef](#)] [[PubMed](#)]
34. Zaragosi, L.E.; Deprez, M.; Barbry, P. Using single-cell RNA sequencing to unravel cell lineage relationships in the respiratory tract. *Biochem. Soc. Trans.* **2020**, *48*, 327–336. [[CrossRef](#)]
35. Ruiz García, S.; Deprez, M.; Lebrigand, K.; Cavard, A.; Paquet, A.; Arguel, M.-J.; Magnone, V.; Truchi, M.; Caballero, I.; Leroy, S.; et al. Novel dynamics of human mucociliary differentiation revealed by single-cell RNA sequencing of nasal epithelial cultures. *Development* **2019**. [[CrossRef](#)]
36. Moser, N.; Mechawar, N.; Jones, I.; Gochberg-Sarver, A.; Orr-Urtreger, A.; Plomann, M.; Salas, R.; Molles, B.; Marubio, L.; Roth, U.; et al. Evaluating the suitability of nicotinic acetylcholine receptor antibodies for standard immunodetection procedures: Evaluation of nicotinic receptor antibodies. *J. Neurochem.* **2007**, *102*, 479–492. [[CrossRef](#)]
37. Rommel, F.R.; Raghavan, B.; Paddenberg, R.; Kummer, W.; Tumala, S.; Lochnit, G.; Gieler, U.; Peters, E.M.J. Suitability of Nicotinic Acetylcholine Receptor  $\alpha 7$  and Muscarinic Acetylcholine Receptor 3 Antibodies for Immune Detection: Evaluation in Murine Skin. *J. Histochem. Cytochem.* **2015**, *63*, 329–339. [[CrossRef](#)]
38. Lam, D.C.-L.; Girard, L.; Ramirez, R.; Chau, W.-S.; Suen, W.-S.; Sheridan, S.; Tin, V.P.C.; Chung, L.-P.; Wong, M.P.; Shay, J.W.; et al. Expression of Nicotinic Acetylcholine Receptor Subunit Genes in Non-Small-Cell Lung Cancer Reveals Differences between Smokers and Nonsmokers. *Cancer Res.* **2007**, *67*, 4638–4647. [[CrossRef](#)]
39. Garg, B.K.; Loring, R.H. Evaluating Commercially Available Antibodies for Rat  $\alpha 7$  Nicotinic Acetylcholine Receptors. *J. Histochem. Cytochem.* **2017**, *65*, 499–512. [[CrossRef](#)]
40. Barrantes, F.J. Cell-surface translational dynamics of nicotinic acetylcholine receptors. *Front. Synaptic Neurosci.* **2014**, *6*. [[CrossRef](#)]
41. Amos, C.I.; Wu, X.; Broderick, P.; Gorlov, I.P.; Gu, J.; Eisen, T.; Dong, Q.; Zhang, Q.; Gu, X.; Vijayakrishnan, J.; et al. Genome-wide association scan of tag SNPs identifies a susceptibility locus for lung cancer at 15q25.1. *Nat. Genet.* **2008**, *40*, 616–622. [[CrossRef](#)] [[PubMed](#)]
42. Hung, R.J.; McKay, J.D.; Gaborieau, V.; Boffetta, P.; Hashibe, M.; Zaridze, D.; Mukeria, A.; Szeszenia-Dabrowska, N.; Lissowska, J.; Rudnai, P.; et al. A susceptibility locus for lung cancer maps to nicotinic acetylcholine receptor subunit genes on 15q25. *Nature* **2008**, *452*, 633–637. [[CrossRef](#)] [[PubMed](#)]
43. Sun, P.; Li, L.; Zhao, C.; Pan, M.; Qian, Z.; Su, X. Deficiency of  $\alpha 7$  Nicotinic Acetylcholine Receptor Attenuates Bleomycin-Induced Lung Fibrosis in Mice. *Mol. Med.* **2017**, *23*, 34–49. [[CrossRef](#)] [[PubMed](#)]
44. Sun, H.-J.; Jia, Y.-F.; Ma, X.-L. Alpha5 Nicotinic Acetylcholine Receptor Contributes to Nicotine-Induced Lung Cancer Development and Progression. *Front. Pharmacol.* **2017**, *8*, 573. [[CrossRef](#)] [[PubMed](#)]
45. Sun, H.; Ma, X.  $\alpha 5$ -nAChR modulates nicotine-induced cell migration and invasion in A549 lung cancer cells. *Exp. Toxicol. Pathol.* **2015**, *67*, 477–482. [[CrossRef](#)] [[PubMed](#)]
46. Bordas, A.; Cedillo, J.L.; Arnalich, F.; Esteban-Rodríguez, I.; Guerra-Pastrián, L.; de Castro, J.; Martín-Sánchez, C.; Atienza, G.; Fernández-Capitan, C.; Rios, J.J.; et al. Expression patterns for nicotinic acetylcholine receptor subunit genes in smoking-related lung cancers. *Oncotarget* **2017**, *8*, 67878–67890. [[CrossRef](#)] [[PubMed](#)]
47. Qian, J.; Liu, Y.; Sun, Z.; Zhangsun, D.; Luo, S. Identification of nicotinic acetylcholine receptor subunits in different lung cancer cell lines and the inhibitory effect of alpha-conotoxin TxID on lung cancer cell growth. *Eur. J. Pharmacol.* **2019**, *865*, 172674. [[CrossRef](#)]

48. Witayateeraporn, W.; Arunrungvichian, K.; Pothongsrisit, S.; Douchawee, J.; Vajragupta, O.; Pongrakhananon, V.  $\alpha$ 7-Nicotinic acetylcholine receptor antagonist QND7 suppresses non-small cell lung cancer cell proliferation and migration via inhibition of Akt/mTOR signaling. *Biochem. Biophys. Res. Commun.* **2020**, *521*, 977–983. [[CrossRef](#)]
49. Friedman, J.R.; Richbart, S.D.; Merritt, J.C.; Brown, K.C.; Nolan, N.A.; Akers, A.T.; Lau, J.K.; Robateau, Z.R.; Miles, S.L.; Dasgupta, P. Acetylcholine signaling system in progression of lung cancers. *Pharmacol. Ther.* **2019**, *194*, 222–254. [[CrossRef](#)]
50. Pillai, S.G.; Ge, D.; Zhu, G.; Kong, X.; Shianna, K.V.; Need, A.C.; Feng, S.; Hersh, C.P.; Bakke, P.; Gulsvik, A.; et al. A genome-wide association study in chronic obstructive pulmonary disease (COPD): Identification of two major susceptibility loci. *PLoS Genet.* **2009**, *5*, e1000421. [[CrossRef](#)]
51. Pillai, S.G.; Kong, X.; Edwards, L.D.; Cho, M.H.; Anderson, W.H.; Coxson, H.O.; Lomas, D.A.; Silverman, E.K. Loci Identified by Genome-wide Association Studies Influence Different Disease-related Phenotypes in Chronic Obstructive Pulmonary Disease. *Am. J. Respir. Crit. Care Med.* **2010**, *182*, 1498–1505. [[CrossRef](#)] [[PubMed](#)]
52. Cho, M.H.; McDonald, M.-L.N.; Zhou, X.; Mattheisen, M.; Castaldi, P.J.; Hersh, C.P.; DeMeo, D.L.; Sylvia, J.S.; Ziniti, J.; Laird, N.M.; et al. Risk loci for chronic obstructive pulmonary disease: A genome-wide association study and meta-analysis. *Lancet Respir. Med.* **2014**, *2*, 214–225. [[CrossRef](#)]
53. The Tobacco and Genetics Consortium Genome-wide meta-analyses identify multiple loci associated with smoking behavior. *Nat. Genet.* **2010**, *42*, 441–447. [[CrossRef](#)] [[PubMed](#)]
54. Douaoui, S.; Djidjik, R.; Boubakeur, M.; Ghernaout, M.; Touil-boukoffa, C.; Oumouna, M.; Derrar, F.; Amrani, Y. GTS-21, an  $\alpha$ 7nAChR agonist, suppressed the production of key inflammatory mediators by PBMCs that are elevated in COPD patients and associated with impaired lung function. *Immunobiology* **2020**, *225*, 151950. [[CrossRef](#)]
55. Bray, M.J.; Chen, L.; Fox, L.; Hancock, D.B.; Culverhouse, R.C.; Hartz, S.M.; Johnson, E.O.; Liu, M.; McKay, J.D.; Saccone, N.L.; et al. Dissecting the genetic overlap of smoking behaviors, lung cancer, and chronic obstructive pulmonary disease: A focus on nicotinic receptors and nicotine metabolizing enzyme. *Genet. Epidemiol.* **2020**, *44*, 748–758. [[CrossRef](#)]
56. Yamada, M.; Ichinose, M. The Cholinergic Pathways in Inflammation: A Potential Pharmacotherapeutic Target for COPD. *Front. Pharmacol.* **2018**, *9*, 1426. [[CrossRef](#)] [[PubMed](#)]
57. Cai, G.; Bossé, Y.; Xiao, F.; Kheradmand, F.; Amos, C.I. Tobacco Smoking Increases the Lung Gene Expression of ACE2, the Receptor of SARS-CoV-2. *Am. J. Respir. Crit. Care Med.* **2020**, rccm.202003-0693LE. [[CrossRef](#)] [[PubMed](#)]
58. Zhang, H.; Rostami, M.R.; Leopold, P.L.; Mezey, J.G.; O’Beirne, S.L.; Strulovici-Barel, Y.; Crystal, R.G. Expression of the SARS-CoV-2 ACE2 Receptor in the Human Airway Epithelium. *Am. J. Respir. Crit. Care Med.* **2020**, rccm.202003-0541OC. [[CrossRef](#)]
59. Wang, Q.; Zhang, Y.; Wu, L.; Niu, S.; Song, C.; Zhang, Z.; Lu, G.; Qiao, C.; Hu, Y.; Yuen, K.-Y.; et al. Structural and Functional Basis of SARS-CoV-2 Entry by Using Human ACE2. *Cell* **2020**, *181*, 894–904.e9. [[CrossRef](#)]
60. Russo, P.; Bonassi, S.; Giacconi, R.; Malavolta, M.; Tomino, C.; Maggi, F. COVID-19 and smoking: Is nicotine the hidden link? *Eur. Respir. J.* **2020**, *55*, 2001116. [[CrossRef](#)]
61. Du Rand, I.A.; Blaikley, J.; Booton, R.; Chaudhuri, N.; Gupta, V.; Khalid, S.; Mandal, S.; Martin, J.; Mills, J.; Navani, N.; et al. British Thoracic Society guideline for diagnostic flexible bronchoscopy in adults: Accredited by NICE. *Thorax* **2013**, *68*, i1–i44. [[CrossRef](#)] [[PubMed](#)]
62. Zuo, W.-L.; Yang, J.; Strulovici-Barel, Y.; Salit, J.; Rostami, M.; Mezey, J.G.; O’Beirne, S.L.; Kaner, R.J.; Crystal, R.G. Exaggerated BMP4 signalling alters human airway basal progenitor cell differentiation to cigarette smoking-related phenotypes. *Eur. Respir. J.* **2019**, *53*, 1702553. [[CrossRef](#)] [[PubMed](#)]
63. Perotin, J.-M.; Coraux, C.; Lagonotte, E.; Birembaut, P.; Delepine, G.; Polette, M.; Deslée, G.; Dormoy, V. Alteration of primary cilia in COPD. *Eur. Respir. J.* **2018**, *52*, 1800122. [[CrossRef](#)] [[PubMed](#)]

